Tumor Biology 45 (2023) 95–110
DOI:10.3233/TUB-220027
IOS Press

Induction of epithelial-mesenchymal transition in thyroid follicular cells is associated with cell adhesion alterations and low-dose hyper-radiosensitivity

Ankit Mathur[a,1], Vijayakumar Chinnadurai[b], Param Jit Singh Bhalla[b,2] and Sudhir Chandna[a,*]

[a]*Division of Radiation Biosciences, Institute of Nuclear Medicine and Allied Sciences, Brig. S.K. Mazumdar Road, Timarpur, Delhi, India*

[b]*Institute of Nuclear Medicine and Allied Sciences, Brig. S.K. Mazumdar Road, Timarpur, Delhi, India*

Received 6 September 2022
Accepted 16 August 2023

Abstract.
BACKGROUND: Epithelial-mesenchymal transition (EMT) is associated with altered cellular adhesion. We previously demonstrated that cellular adhesion influences Low-dose Hyper-Radiosensitivity (HRS) in a variety of tumor cells. However, the relationship of low-dose HRS with the phenotypic plasticity incurred by EMT during the neoplastic transformation remains to be elucidated.
OBJECTIVE: To investigate whether acquisition of EMT phenotype during progressive neoplastic transformation may affect low-dose radiation sensitivity.
METHODS: Primary thyroid cells obtained from a human cystic thyroid nodule were first subjected to nutritional stress. This yielded immortalized INM-Thy1 cell strain, which was further treated with either multiple γ-radiation fractions (1.5 Gy each) or repetitive cycles of 3-methylcholanthrene and phorbol-12-myristate-13-acetate, yielding two progressive transformants, viz., INM-Thy1R and INM-Thy1C. Morphological alterations, chromosomal double-minutes, cell adhesion proteins, anchorage dependency, tumorigenicity in nude mice and cellular radiosensitivity were studied in these strains.
RESULTS: Both transformants (INM-Thy1R, INM-Thy1C) displayed progressive tumorigenic features, viz., soft agar colony growth and solid tumor growth in nude mice, coupled with features of epithelial-mesenchymal transition and activated Wnt pathway. Incidentally, the chemical-induced transformant (INM-Thy1C) displayed a prominent HRS ($\alpha_s/\alpha_r = 29.35$) which remained unaffected at high cell density. However, the parental (INM-Thy1) cell line as well as radiation-induced transformant (INM-Thy1R) failed to show this hypersensitivity.
CONCLUSION: The study shows that induction of EMT in thyroid follicular cells may accompany increased susceptibility to low-dose ionizing radiation, which was attenuated by adaptive resistance acquired during radiation-induced transformation.

Keywords: Epithelial-mesenchymal transition, low-dose hyper-radiosensitivity, cell adhesion, neoplastic transformation, primary thyroid cells

[1]Current Address: Delhi School of Public Health, Institution of Eminence, University of Delhi, Delhi.

[2]Current Address: House No. 6, Phase I, Housing Board Colony, Baddi, Himachal Pradesh-173205, India.

*Corresponding author: Sudhir Chandna, Division of Radiation Biosciences, Institute of Nuclear Medicine and Allied Sciences, Brig. S.K. Mazumdar Road, Timarpur, Delhi-110054, India. E-mails: sudhirchandna@inmas.drdo.in; sudhirchandna@yahoo.com.

1. Introduction

Human tumor cell lines generally display varying levels of low-dose hyper-radiosensitivity (HRS) characterized by reduced cell survival typically at ionizing radiation doses below 50cGy [1, 2]. Since normal cells have failed to display this unusual phenomenon with the same propensity [3, 4], it is proposed that acquisition of transformed characteristics as well as alterations in cell-cell/cell-matrix interaction may influence low-dose radiation responses [5, 6]. However, cellular radiation responses at low doses have not been studied so far in a controlled transforming cell system. Therefore, we have attempted to evaluate low-dose γ-radiation sensitivity at successive stages of *in vitro* epithelial-mesenchymal transition during neoplastic transformation, using human thyroid follicular cell system. Thyroid cancer is a very common endocrine-related malignancy, with global incidence rising exponentially over the last few decades [7, 8]. Although thyroid cancers are rarely fatal, their recurrence rate is rather high among different carcinomas [9]. The multiple risk factors for thyroid carcinomas include dietary [10] and genetic factors [11]. Incidentally, radiation is a well-established causal agent of thyroid cancer [12], and has a high risk following radiotherapeutic treatment of head and neck cancers [13]. Very limited experimental *in vivo* and *in vitro* models are in place to gain insight into the mechanisms of thyroid carcinogenesis, which remain of concern till date.

In the present study, we conducted *in vitro* transformation of human primary thyroid follicular cells isolated from fine needle aspirates of a euthyroid subject. The initial immortalized cell strain was further transformed either by γ-radiation alone or chemical carcinogen treatment (cycles of 3-methylcholanthrene (3-MCA) along with phorbol 12-myristate 13-acetate (PMA)). Alterations in the radiosensitivity of cell strains demonstrating distinct tumorigenic potential during progressive stages of transformation were studied. Since cell adhesion mechanisms are also crucial to overall response against external stimuli and greatly influence the therapeutic outcome [14], alterations in expression levels of few key proteins were also assessed. The study shows interesting differences in the low-dose radiosensitivity following chemically-induced neoplastic transformation compared to radiation-induced transformation.

2. Material and methods

2.1. Cell culture and in vitro transformation

A primary human thyroid cell culture was established using fine-needle aspirated (FNA) cells from a 40-year-old female patient with symptoms of thyroid goiter, after obtaining the necessary approval of the study from the institutional human ethics committee (no. IIHEC/CT/2017/20). Primary cells and the transformants were maintained as a monolayer at 37°C in Dulbecco's modified Eagle's medium (Sigma-Aldrich, StLouis, MO, USA), supplemented with 5% fetal bovine serum (Gibco, Carlsbad, CA, USA) and antibiotics (Penicillin, 50,000 Units/L, Streptomycin-100 mg/L).

For oncogenic transformation, these primary thyroid cells were subjected to nutritional deprivation for 3 weeks without replenishing growth medium. A single cell clone (INM-Thy1) was derived from the resulting cell population through dilution cloning. Morphological features, such as overall size (length/width ratio) and substrate attachment area of an individual strain was monitored over time. These features were found to be stable through multiple passages in culture. From this strain, further transformation was carried out by two different methods (Fig. 2A), i.e., by repeated γ-irradiation (1.5 Gy) during logarithmic growth phase of 23 sequential passages (total dose = 34.5 Gy), or by application of alternate cycles of 3-methylcholanthrene (3-MCA; 5 μg/mL) and phorbol 12-myristate 13-acetate (PMA; 0.05 μg/mL) at 24 h interval for 13 sequential passages. These treatments finally yielded transformed cell strains named INM-Thy1R and INM-Thy1C, respectively.

2.2. Anchorage independence assay

Anchorage independence was assayed as previously described [15]. Briefly, 50,000 cells/ 60 mm Petri dish were resuspended in 0.33% agarose overlaid on a layer of 2% agarose and covered with fresh growth medium. The growth of 500 randomly selected colonies from different planes in the soft agar layer was measured after three weeks under Axiovert 200 DIC microscope (Carl Zeiss, Oberkochen, Germany). Colony size was evaluated by measuring two orthogonal diameters (d1/d2) using the AxioVision Rel.4.8 software. The volume was calculated using the formula $V = 4/3\ \Pi r^3$, where $r = 1/2\sqrt{}d1d2$ is the geometric mean radius.

2.3. Tumorigenicity in nude mice

As described earlier, the tumorigenic potential of the cells was assessed by inoculating the cells in nude mice [16]. We standardized the protocol by inoculating various number of cells in 100 µl PBS and found the optimum concentration to be 6 million the INM-Thy1 cells for the appearance of palpable tumors. Briefly, exponentially growing cells were inoculated subcutaneously into the scapular region of nude mice aged 6 to 10 weeks. Tumors forming a palpable nodule at the site of injection were measured up to 10 weeks/permissible maximum size. Animal experiments were approved by the institutional animal ethical committee (INM/IAEC/16/24).

2.4. Cell survival assay

Radiation dose response of all cell strains was assessed using macrocolony (survival) assay as described earlier [1]. Briefly, asynchronously growing cells were first plated at low density (5-6 cells/cm^2), 18–24 h prior to γ-irradiation using ^{60}Co source (1.034 Gy/min; Teletherapy Unit, Bhabhatron-II, Panacea Medical Technology, Bangalore, India). Cultures were maintained at 37°C in a humidified incubator with 95% air/5% CO_2 for 5–7 days before fixing and staining with 1% crystal violet. Colonies with >50 cells were counted for calculating plating efficiency with respect to untreated control. For irradiation at high cell density, ∼35,000–40,000 cells/cm^2 were irradiated at varying doses and plated at a density of 5-6 cells/cm^2 for macrocolony formation. Each experiment was repeated at least three times with triplicate samples.

2.5. Wound healing (cell migration) assay

Wound healing assay was performed to assess alterations in cell migration as described earlier [17]. Briefly, semi-confluent cultures grown in Petri dishes were scraped using sterile microtip, rinsed twice with PBS and supplemented with fresh growth medium containing reduced serum concentration (5%). To standardize the gap and the observation time, the time taken for the most migrating cells (INM-Thy1) to cover ∼50% of the gap was taken as a reference time. Images were captured in multiple spots along the wound using Axiovert-200 Zeiss inverted microscope (Carl Zeiss) immediately or 8 h after scraping. The total distance of cell migration was calculated by measuring the distance between the two leading edges of the wound.

2.6. Western blotting

Western blotting was performed for assessing alterations in protein expression as described earlier [17]. Anti-E-Cadherin (sc-7870;1:1000; Santa Cruz Biotechnology, Santa Cruz, CA, USA), anti-β-catenin (sc-7199; 1:1000; Santa Cruz Biotechnology), anti-phospho-β-catenin (9566, Cell

Signalling Technologies), anti-integrinα_v (611013; 1:500; BD Biosciences, San Jose, CA, USA), anti-connexin43(6219; 1:1500; Sigma-Aldrich), anti-β-actin (sc-1615;1:1000; Santa Cruz Biotechnology), and anti-vimentin (550513; 1:1000; BD Biosciences) antibodies were used along with a chemiluminescence detection system (Thermo Scientific, Waltham, MA, USA). ImageQuant system (GE Healthcare, Little Chalfont, United Kingdom) was used for quantification.

2.7. Immunofluorescence microscopy

Intracellular protein localization was detected using immunoflorescence microscopy [18]. Anti-β-catenin antibodies were used along with FITC-conjugated secondary antibodies. Images were captured at 63X magnification (oil immersion) and processed using fluorescence imaging system (Axio-Imager M2; AxioVision Rel.4.8; Carl Zeiss). Nuclear beta-catenin localization was quantified by measuring mean florescence intensity of the nuclear region of the cells labelled with FITC. Fifty randomly selected cells from at least 10 different regions of three independent experiments were measured using the Zen2.3 pro software.

2.8. Chromosomal analysis

Metaphase spreads of exponentially growing cells were prepared according to the standard procedure [19]. Images of Giemsa-stained chromosomes were captured at 100X magnification (oil) using Axio-Imager M2 (Carl Zeiss). At total of 100 well spread metaphases with distinct chromosome morphology were selected for the analysis of numerical and specific structural aberrations.

2.9. Growth kinetics

Exponentially growing 3×10^5 cells were inoculated in a 60 mm Petri dish. Subsequently, every 24 hours the cells were harvested from monolayer and counted under a phase contrast using hemocytometer/ automated cell counter.

2.10. Cell survival analysis through LQ and IR models

A MATLAB-based script was developed to estimate dose/surviving fraction dependencies through linear-quadratic (LQ) formalism and further enhanced with an induced repair (IR) model. The LQ model was fitted as

$$\text{Survival Fraction (SF)} = \exp(-\alpha + \beta D^2) \pm \mu$$

Where D is the radiation dose in Gy, on the log-linear plot of survival curve, α is the cell kill per Gy of the linear component, and β is the cell kill per Gy^2 of the quadratic component.

Furthermore, the IR model [20] was fitted to delineate cell survival as functions of two separate α components, viz., α_s and α_r,

$$SF = \exp(\alpha_r \; D\{1 + (\alpha_s \,/\, \alpha_r - 1)\exp(-D/DC)\} - \beta D^2)$$

IR model very well fits the HRS curve that depicts transition from sensitive to resistant response at the immediately higher doses (the region of induced radioresistance/ IRR). 'Dc' is depicted as the transition point between HRS and IRR regions. The script carried out a nonlinear fitting based on nonlinear least square, using Trust-region algorithm as the optimizer. The coefficient of determination (R^2) was estimated as goodness of the fit measure and was set to 0.95(=95%) level of certainty.

2.11. Statistical analysis of data

Wherever necessary, differences in the mean (±SD) values of different treatments were analysed for significance using the unpaired two-tailed Student's *t*-test for independent samples.

3. Results

3.1. Nutritional crisis in primary thyroid cells resulted in transformed cells with altered morphology and growth characteristics

Fine-needle aspirated primary human thyroid cells cultured in a complete growth medium, after four days formed an organized assembly of follicular structures, resembling classical epithelial morphology. The majority of cells retained the typical morphology of differentiated thyroid follicular cells for the subsequent two weeks in culture, even when their growth was restricted (Fig. 1A). Cells with fibroblast morphology were rarely observed, and were eliminated during the nutritional crisis phase.

In order to induce malignant transformation, these follicular cells were maintained in nutrition-deprived condition by not replacing growth medium for three weeks, which resulted in a significant reduction of adherent cells on the surface of the flask. The remaining live floating cells were subsequently reintroduced into a fresh growth medium. With time, a small proportion of the floating cells attached to the bottom of the flask, and by the twelfth week, adherent cells formed a rapidly proliferating monolayer. This cell population had more elongated spindle-shaped morphology than the parental primary follicular cells, as indicated by a higher length/width ratio (Fig. 1B). A relatively lower surface-attached area (Fig. 1C), along with the induction of rapid growth in the resultant population as compared to the parental cells, suggests the induction of oncogenic transformation in the primary follicular cells. Clonal isolation of the transformed cells carried out by dilution cloning yielded a single cell clone named 'INM-Thy1'.

3.2. Radiation or chemical carcinogen treatment induced further transformation of 'INM-Thy1' cells with distinct morphological alterations

INM-Thy1 cells were further subjected to two different modes of cell transformation (Fig. 2A). Firstly, cells were γ-irradiated at 1.5 Gy dose fractions repeated 23 times (total dose = 34.5 Gy), at each subsequent passage during exponential growth phase of culture. At the end of this treatment, the majority of the resulting cells exhibited more flattened fibroblast-like morphology than the parental INM-Thy1cells (Fig. 2B) which has remained stable during for over 100 subsequent passages, confirming a stable transformation of cells. The resulting cell strain was named as 'INM-Thy1R'. These cells exhibited morphological features similar to fibroblast cells with the cell size (Fig. 2C) and surface attachment area (Fig. 2D) drastically increased compared to the preceding strain, INMThy1.

Secondly, cells were treated in alternate cycles with a potent carcinogen, 3-MCA, and tumor promoter, PMA, administered at each log phase during sequential passages. This resulted in another stably transformed cell strain 'INM-Thy1C', with relatively more elongated, spindle-shaped morphology and enhanced cell protrusions compared to the parental INM-Thy1 cells (Fig. 2B), indicating an acquisition of mesenchymal features in these transformants. However, neither of these two transformants had any significant alterations in growth potential as compared to the parental cell strain, as indicated by unaltered population doubling time (Fig. 2E).

Since double minutes are frequently encountered in cancer cells (Gebhart et al. 1984), we analysed metaphase spreads of INM-Thy1 and its transformants (Fig. 2F). Interestingly, the proportion of cells

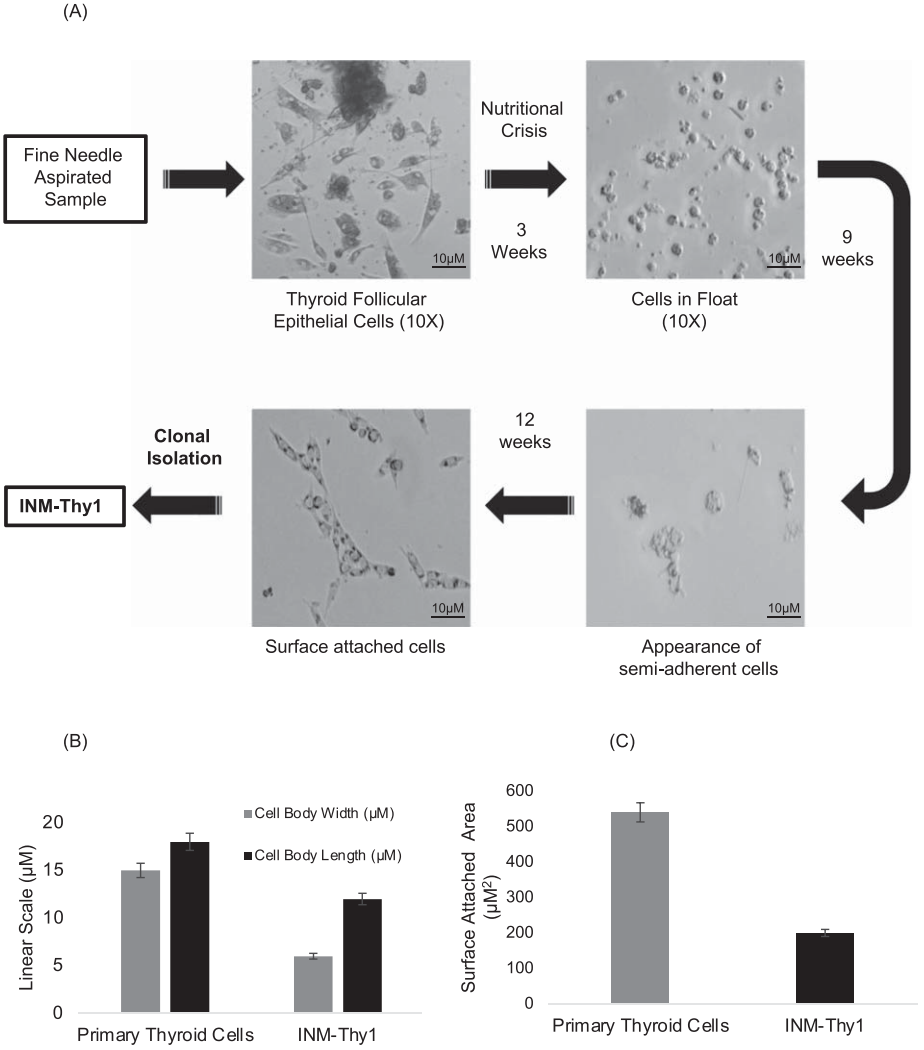

Fig. 1. *In vitro* nutritional deprivation to primary thyroid cells yields an aneuploid transformant: (a) DIC photomicrographs depicting establishment of various stages of *in vitro* transformation of thyroid primary cells (magnification 10X). (b) Length/width measurements of the primary thyroid and transformed cells. 500 randomly selected cells were measured from at least 20 microscopic images. Measurements were carried out using AxioVision Rel 4.8 software. (c) Area of cell-substrate attachment of 500 randomly selected cells to the tissue culture flask. The periphery of individual cell was measured using AxioVision Rel 4.8 software to calculate the area of attachment.

with double minutes increased markedly in the two later transformants as compared to the parental INM-Thy1 strain (Table 1). INM-Thy1C also had significantly reduced mean chromosome number (31 ± 6.99; $p = 0.014$) when compared to the parental (INM-Thy1) and INM-Thy1R strains.

3.3. Transformed INM-Thy1R and INM-Thy1C cells have higher tumorigenic potential and reduced cell migration rate

Anchorage independency of all three 'INM-Thy' strains was assessed using soft agar assay. Interestingly, all transformed cell strains were able to form colonies in soft agar with varying efficiency (Fig. 3A). However, radiation-induced (INM-Thy1R) and chemically-induced (INM-Thy1C) transfor-

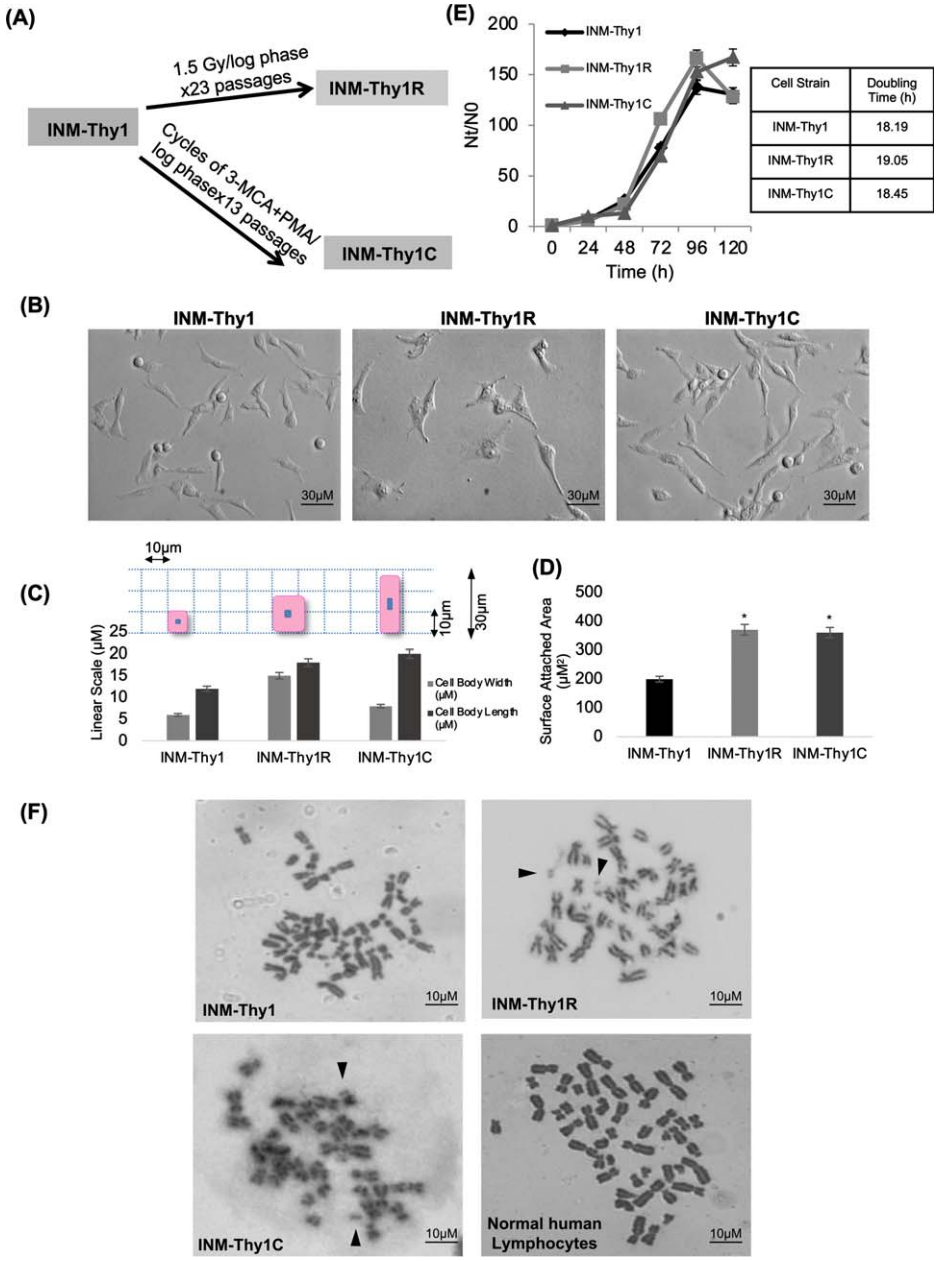

Fig. 2. (a) Schematic representation of method of development of radiation (INM-Thy1R) and chemical induced transformants (INM-Thy1C) from INM-Thy1 cells. (b) DIC photomicrograph showing contrasting morphology of INM-Thy1 and its transformants. Equal number of cells were seeded and images were captured 24 h post seeding (magnification 20X). (c) Morphological variation represented as overall size of the individual cell strain. Following 24 h post seeding, the length/width of 500 randomly selected cells from a least 20 images were measured using AxioVision Rel 4.8 software. A cartoon illustration (on top of graph) depicts the cell size. (d) Area of cell-substrate attachment to the tissue culture dish was measured by inoculating 0.8×10^6 cell/PD_{60}. DIC images were captured 24 h post seeding and surface-attached area of randomly selected 500 cells was measured using AxioVision Rel 4.8 Software. (e) Proliferation kinetics of exponentially growing cells in culture. Each point represents data from three independent experiments. (f) Representative phase contrast images of Giemsa-stained metaphase spread of INM-Thy1 and its transformants (magnification 100X). Chromosomal double minutes are shown by arrow heads. Normal human lymphocytes were taken as control. Table 1 shows quantitative analysis of types of aberrations obtained from 100 spreads of INM-Thy1 cells.

Table 1
Chromosomal imbalance in INM-Thy1 and its Transformants

Strain	Mean number of chromosomes/cell	Mean number of double minutes/ cell
INM-Thy1	37.74 ± 8.9	0
INM-Thy1R	38.46 ± 7.82 $P = 0.25$	0.37
INM-Thy1C	31 ± 6.99 $p = -0.014$	0.27

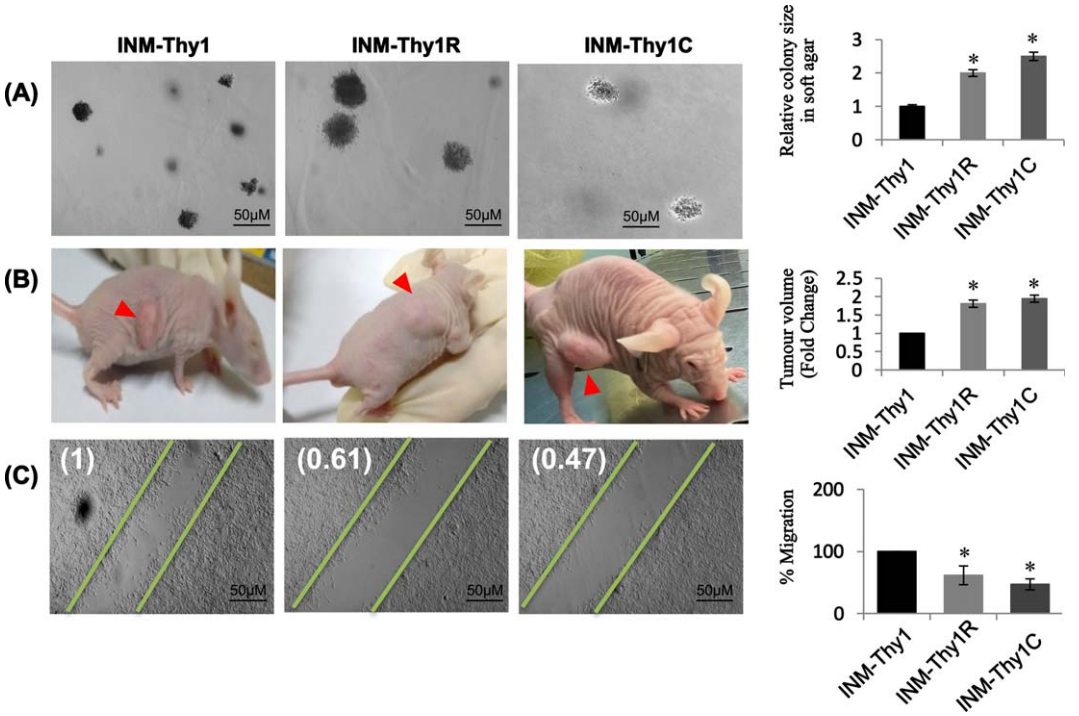

Fig. 3. Higher tumourigenic potential in transformed cells characterized by increased tumour forming ability and reduced cell migration: (a) Phase contrast images (5X) of soft agar colony formation assay to test anchorage independence of INM-Thy1 and transformed strains (Mean ± SE of three observations from three independent experiments; $^{*}p < 0.05$). Graphical representation of relative colony size of 500 randomly selected colonies from different planes of soft agar layers (right panel). Data represent three individual experiments performed in triplicates. (b) In *vivo* tumourigenic assay photographs of the tumours (red arrowheads) and animals were taken 4 weeks post inoculation. Tumour volumes normalized with parental INM-Thy1 strain from three independent experiments are shown (right panel) ($^{*}p < 0.05$). (c) DIC images of wound healing assay to analyse cell migration 8 h after scraping. Corresponding fold migration is indicated at top left corner of each image. Data (mean ± SD) are presented after normalizing with respect to parental INM-Thy1 cells from three independent experiments.

mants showed a 2.5-fold higher colony growth rate than the parental INM-Thy1 cells, suggesting an increase in anchorage independence with progressive transformation (Fig. 3A).

The *in vivo* tumorigenic potential of all strains was evaluated by subcutaneous implantation into nude mice. All the three transformants were able to form xenograft tumor at the site of inoculation, with a comparable latency period (~10 days) before appearance of palpable tumor mass. However, the

growth of the tumor arising from the INM-Thy1 strain was found to be comparatively slower even after a long incubation period of 30 days, as compared to INM-Thy1R and INM-Thy1C cells, suggesting a higher tumorigenic potential in these two latter strains (Fig. 3B).

The wound healing assay detected significant reduction in cell migration by up to 53% in INM-Thy1R and INM-Thy1C cells, compared to the parental INM-Thy1 strain (Fig. 3C).

3.4. Altered expression of cell adhesion molecules and activated Wnt signalling in INM-Thy1R and INM-Thy1C cells

We further analysed the expression of six cell adhesion proteins known to be associated with tumorigenicity. The adherence junction protein, E-cadherin, was found marginally overexpressed in both INM-Thy1R and INM-Thy1C cells (Fig. 4A), while its associated protein, β-catenin, a functional component of the Wnt signaling pathway, was considerably upregulated by ∼2.5 fold. Immunofluorescence imaging, in both of these strains, detected a nuclear localization of β-catenin (Fig. 4B, C), which was in complete contrast to the cytoplasmic distribution in the parental INM-Thy1 cells (Fig. 4C). To quantify the nuclear localization of β-catenin we measured the mean fluorescence intensity of FITC in the nuclear region of 50 cells from at least 10 images from three independent experiments. We found ∼2 fold increased β-catenin signals in the INM-Thy1C and INM-Thy1R cells compared to the parental cell strain INM-Thy1 (right panel). Stabilization of β-catenin mediated by a specific de-phosphorylation is considered a prerequisite for Wnt pathway activation. Incidentally, significant dephosphorylation of β-catenin was observed in INM-Thy1R (∼2 fold) as well as INM-Thy1C (∼4 fold) compared to the parental cells, thereby strongly indicating Wnt activation in both the latter transformants, apparently having a higher tumorigenic potential (Fig. 3B). The translocation of β-catenin into the nucleus further confirms the activation of Wnt pathway in the two latter strains, corroborating the protein expression alterations observed by Western blots (Fig. 4B). Integrin-α_v, which mediates communication through extracellular matrix and can facilitate tumor progression, remained unchanged in all three cell strains (Fig. 4A). Interestingly, however, the P0 and P1 bands of phosphorylated Cx43 [21] were found to be of considerably higher intensity (∼3 fold) in the latter two transformants (Fig. 4A). Vimentin, an intermediate filament family of proteins established as a marker of epithelial-mesenchymal transitions (EMTs), was also considerably upregulated in both the INM-Thy1R and INM-Thy1C strains. Morphological alterations, upregulated vimentin expression and activated Wnt pathway indicate acquisition of EMT like phenotype in two latter transformats.

It is to be mentioned that in this system, EMT was not achieved to an advanced stage, as both transformants lacked some mesenchymal characteristics. For example, the downregulation of E-cadherin was not significant in either of the two transformed strains (INM-Thy1C, INM-Thy1R). The lack of completion of EMT was evidently associated with the lack of invasive phenotype, as indicated by reduced migration of both these transformed strains (Fig. 3C). Thus, this thyroid transformation model represents a transformation with enhanced tumorigenic potential and partial mesenchymal characteristics.

3.5. Low-dose hyper-radiosensitivity was selectively expressed in chemically-transformed INM-Thy1C cell strain

As stated above, the induction of low-dose HRS has been observed more prominently in tumor cells than normal cells, and cell-cell contact is also known to influence low-dose hyper-radiosensitivity [1]. We thus analyzed radiation dose response of all three transformants using macrocolony assay, which was performed by irradiating pre-plated cells at sparse cell density (5-6 cells/cm^2) (Fig. 5A) or irradiating high density cultures (∼35,000–40,000), followed by plating (Fig. 5B). The cell survival

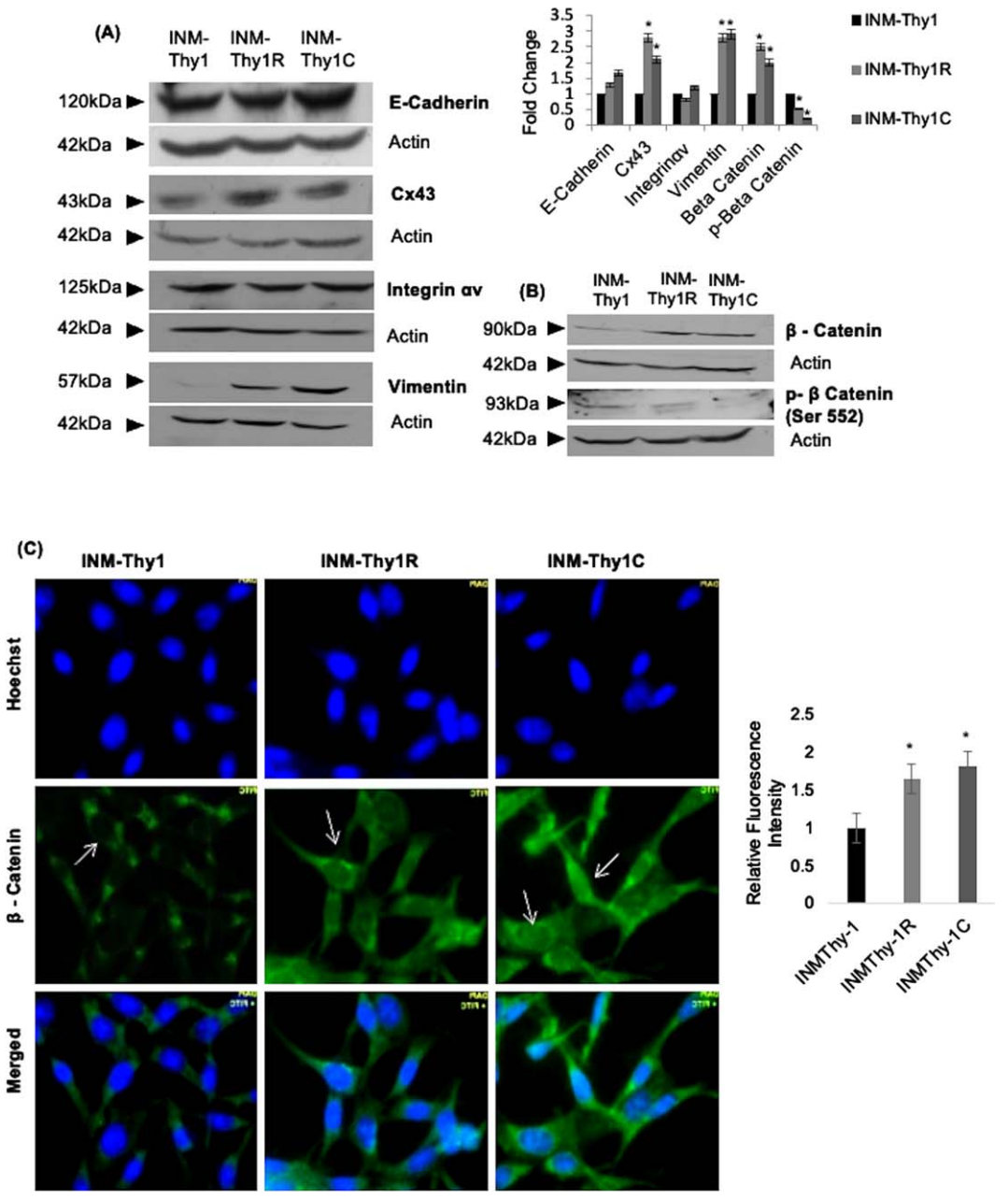

Fig. 4. Alterations in expression and intracellular localization of cell adhesion proteins following transformation: (a) Western blot analysis of the expression of the indicated cell adhesion proteins. Representative blots and densitometry of protein bands relative to β-actin from three independent experiments are shown ($^*P \leq 0.05$). (b) Representative western blots of β-catenin and phospho- β-catenin indicate activation of Wnt pathway in the transformed cells. (c) Immunofluorescence images showing intracellular localization (arrows) of β-catenin (magnification 63X). Relative fluorescence intensity of FITC-labeled nuclear region of the three cell strains, representing nuclear localization of β-catenin (right panel). A total of 50 randomly selected cells from at least 10 images per strain were analysed using Zen 2.3 pro software. Representative images of three independent experiments are shown.

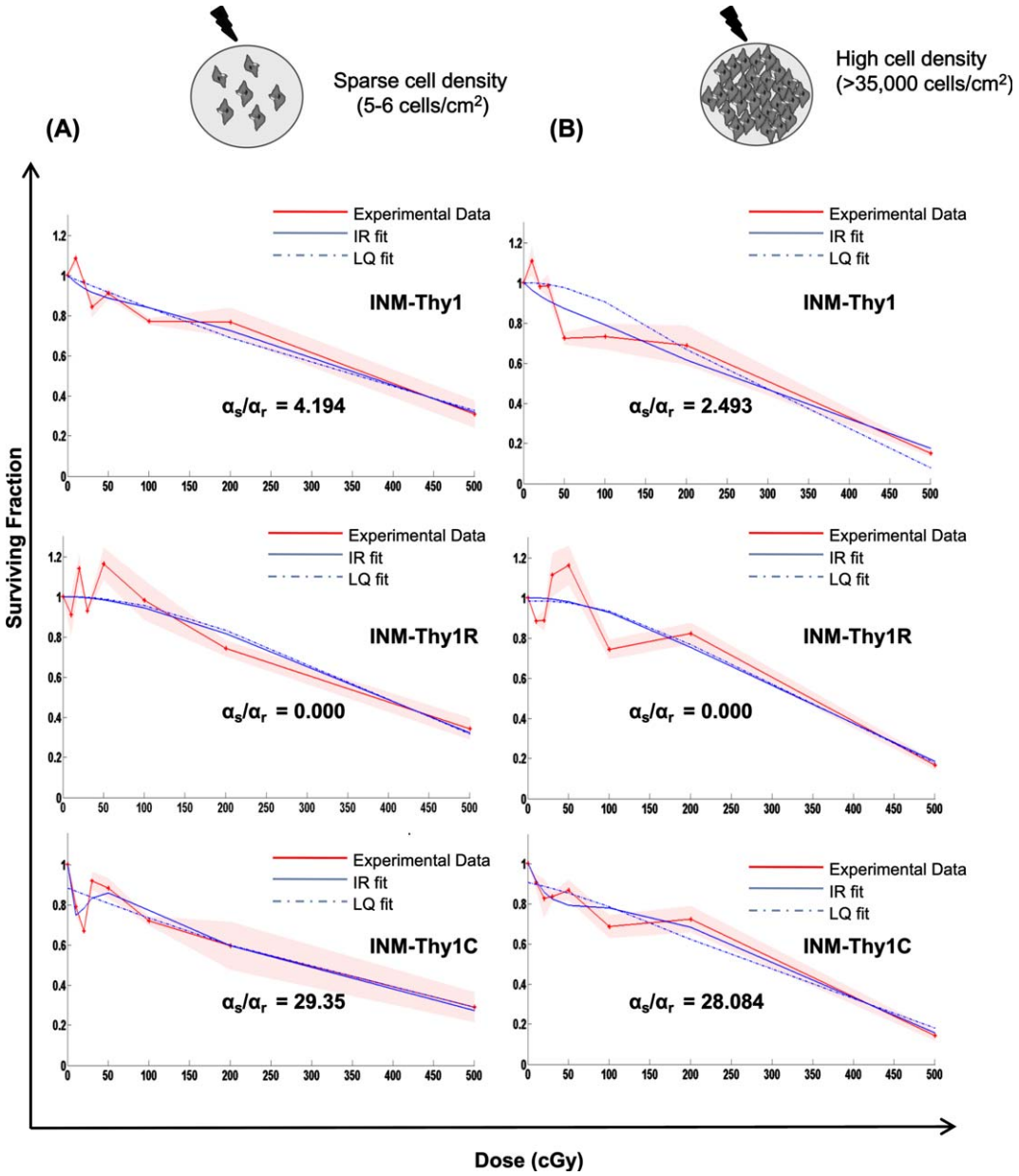

Fig. 5. Low-dose radiation survival dose response under sparse cultures v/s high cell density: Clonogenic cell survival dose response of the parental INM-Thy1 and transformed strains (INM-Thy1R and INM-Thy1C), when cells were plated at low (a) and high (b) cell density. The survival curve was fitted to the LQ (dotted blue line) and IR (smooth blue line) models, along with the experimental data (smooth red line), the respective α_s and α_r values are shown. Each data point is the mean of nine observations from three independent experiments, and the color shade represents standard deviation.

curve for parental INM-Thy1 cells and its radiation-induced transformant (INM-Thy1R) showed dose-dependent reduction in surviving fraction up to 5 Gy. As shown in Fig. 5A and B, the close proximity of the survival curve fits for both LQ and IR models, and indicates the lack of induction of HRS in both cell strains. In the chemical-induced transformant INM-Thy1C (Fig. 5A), radiation dose-response curve deviated from LQ model and displayed steep reduction in surviving fraction (SF) at the doses of up to 20cGy ($SF_{0.1Gy} = 0.70 \pm 0.22$), even as SF recovered at the immediately higher doses of up

to 50cGy ($SF_{0.5Gy} = 0.80 \pm 0.16$). The ratio of the slope obtained in the low-dose region (α_s) with the slope obtained from linear-quadratic fit of the high-dose data (α_r), which estimates the fold-increase in radiosensitivity specificaly at low-doses, was markedly higher ($\alpha_s/\alpha_r = 29.35$) compared to the other two strains. The transition point between HRS and IRR referred to as Dc [1] was found at 9.8 cGy for INM-Thy1C cells. The IR model further confirmed the occurrence of HRS in the chemical-induced transformant INM-Thy1C, even when cells were irradiated at high density (Fig. 5B).

4. Discussion

Progressive transformation of cells may involve several phenotypic alterations, including altered morphology, cellular adhesion/communication and mobility, or karyotypic heterogeneity [22, 23]. In the present study, nutritional deprivation of primary human thyroid follicular cells followed by chemical carcinogen or radiation exposure gave rise to multiple cellular strains that reflect progressive stages of tumor development. Nutritional deprivation of normal primary thyroid cells generated morphologically distinct population of cells with enhanced growth potential and marked variation in chromosomal numbers. The induction of aneuploidy often leads to an overall altered cell physiology, including defects in cell proliferation that may lead to immortalization [24], anchorage-independent growth [25], and tumorigenicity in some cases [26]. The chromosomal imbalance in INM-Thy1 cells corresponded with the acquisition of these diverse characteristics (Figs. 2 and 3). Accumulated metabolites and reduced pH during the deprivation might be the strongest causative factors associated with this event, as previously established by studies on different cell types [27, 28] and animal models [29].

Two complimentary approaches were used to further transform the parental INM-Thy1 cells. Repetitive exposure to either radiation or chemical carcinogen not only resulted in enhanced anchorage independence, but also increased tumorigenic potential, as evidenced in INM-Thy1R and INM-Thy1C cells. Since the presence of double minutes may impart selective advantage for growth and survival, the occurrence of double minutes in the two latter strains may be associated with enhanced tumorigenic potential. Surprisingly, unlike most reported studies with similar transformation approaches, these advanced cell strains showed reduced cell motility even though their growth potential remained unchanged despite the activation of the Wnt pathway. These data suggest that the acquisition of increased tumorigenic potential may not necessarily be associated with a higher proliferation rate, resembling the mild nature of most of the commonly occurring thyroid malignancies [30, 31]. It is noteworthy that the patient from whom the thyroid cells were isolated turned out to be a euthyroid patient. The study indicates the possibility of a premalignant disposition in follicular cells of this donor, since nutrient deprivation yielded transformed cells in the first attempt. While samples were also taken from multiple patients, the success rate of establishing and immortalizing/transforming primary cells is known to be quite low (data not shown). Therefore, the study holds relevance for elucidating the mechanisms of carcinogenesis and understanding alterations in radiosensitivity with progressive changes in this process.

In line with distinct morphological alterations, certain cell adhesion molecules were also found to be altered in strains with higher tumorigenic potential, namely in INM-Thy1R, INM-Thy1C. Firstly, both of the aggressively transformed strains exhibited marginal overexpression of E-cadherin, an adherence junction protein known to maintain apico-basal polarity [32] and actin cytoskeletal dynamics [33], which can be correlated to the reduced migratory property in the latter transformants (Fig. 3C). Interestingly, both of these transformed strains showed a significant increase in the mesenchymal marker vimentin, along with the activation of the Wnt pathway, suggesting enhanced tumorigenic potential typically associated with the EMT process. Gap junctional protein Cx43 was also found to be upregulated in INM-Thy1R and INM-Thy1C strains, thus supporting its complex and dynamic

behaviour at different stages of cancer development [34]. The cell-ECM interacting protein Integrin α_v remained unaltered amongst all the transformed strains. More recently, the plasticity of epithelial to mesenchymal states is considered as a non-binary switch, where a subgroup of cells may linger in an intermediate state and co-exhibit mesenchymal as well as epithelial markers, a phenomenon termed as partial EMT (p-EMT) [35, 36]. Thus, the thyroid transformation model in the current study also exhibits certain EMT characteristics of transforming cells. Similar intermediate states were also obtained in one of our studies in which we established multiple stages of progressive MET in NIH3T3 fibroblasts [6].

It is quite interesting that a distinct induction of low-dose HRS was explicitly displayed by the chemically induced transformant (INM-Thy1C), whereas the parental strains INM-Thy1 and its radiation-induced transformant INM-Thy1R failed to show a similar response at low doses. Furthermore, HRS was not diminished in INM-Thy1C cells under conditions of high cell density, unlike in our previously published studies on tumor cells [1] and cells undergoing mesenchymal-epithelial transition [6]. The low-dose HRS is a common phenomenon shown in a variety of tumor cells [37, 38]. However, the extent to which it appears varies in cells with different origins, tumor grades and genetic backgrounds. As previously demonstrated by us and other groups, cells with high proliferative potential, e.g. human glioma cells, have distinctly higher sensitivity to low doses of radiation as compared to other tumorigenic cells [1, 38]. During carcinogenesis, a spectrum of cells with different cell surface characteristics, gene expression and cellular repair efficiencies exhibit altered sensitivity to low doses of radiation. The current study, involving cells with phenotypic plasticity and low-dose radiosensitivity, is in line with our previously published data, demonstrating variable sensitivity of cells undergoing mesenchymal-epithelial transition [6]. Collectively, we hypothesize that the sensitivity to low doses of radiation is context-dependent and cell type-specific, and may be influenced by various genetic and/or epigenetic factors incurred during carcinogenesis. The absence of HRS in radiation-induced transformant INM-Thy1R, even following irradiation at sparse cell density, may be explained by adaptive radioresistance acquired during radiation-induced transformation. This *in vitro* transformation study with thyroid follicular cells suggests that during thyroid tumor progression, cells may acquire a mild increase in intrinsic low-dose radiosensitivity, which was incidentally suppressed by radiation-induced adaptation. During external beam radiotherapy of cervical region, the thyroid is considered an organ at risk, receiving sub-lethal doses of γ-radiation [39]. The study thus suggests differential low-dose radiation response of sporadic v/s low-dose radiation-induced thyroid malignancies which may necessitate corresponding treatment modalities and an enhanced intensity of screening. In combination with the concomitant activation of the Wnt pathway, the radiation and chemical stress responses observed herein may provide better insights into the molecular pathogenesis of thyroid carcinomas, ultimately contributing to improved therapeutics.

Acknowledgments

This work was done as a part of the project grant DRDO-INM-311-1- 5 of the Defence Research and Development Organisation (DRDO), Ministry of Defence, India. AM thanks the Council of Scientific and Industrial Research (CSIR) for receiving research fellowship.

Author contributions

CONCEPTION: Ankit Mathur, Sudhir Chandna.
DATA CURATION: Ankit Mathur, Sudhir Chandna, Param Jit Singh Bhalla.
ANALYSIS OF DATA: Ankit Mathur, Sudhir Chandna, Vijayakumar Chinnadurai.

PREPARATION OF THE MANUSCRIPT: Ankit Mathur, Sudhir Chandna.

REVISION FOR IMPORTANT INTELLECTUAL CONTENT: Ankit Mathur, Sudhir Chandna, Param Jit Singh Bhalla.

SUPERVISION: Sudhir Chandna.

Conflict of interest

The authors declare that they have no conflicts of interest.

Ethical considerations

All procedures performed in this study involving human participants and animals were approved by the institutional human (IIHEC/CT/2017/20) and animal (INM/IAEC/16/23) ethical committees. All applicable international, national and/or institutional guidelines for the care and use of animals were followed.

Funding

The study was funded by the project grant DRDO-INM-311-1-5 of the Defence Research and Development Organisation (DRDO), Ministry of Defence, India. AM received fellowship and contingency grants from the Council of Scientific and Industrial Research (CSIR), Government of India.

References

[1] Chandna S, Dwarakanath BS, Khaitan D, Mathew TL, Jain V. Low-dose radiation hypersensitivity in human tumor cell lines: Effects of cell-cell contact and nutritional deprivation. Radiat Res. 2002;157(5):516-25. DOI: 10.1667/0033-7587(2002)157[0516:ldrhih]2.0.co;2

[2] Marples B, Collis SJ. Low-dose hyper-radiosensitivity: Past, present, and future. Int J Radiat Oncol Biol Phys. 2008;70(5):1310-8. DOI: 10.1016/j.ijrobp.2007.11.071

[3] Thomas C, Charrier J, Massart C, Cherel M, Fertil B, Barbet J, et al. Low-dose hyper-radiosensitivity of progressive and regressive cells isolated from a rat colon tumour: Impact of DNA repair. Int J Radiat Biol. 2008;84(7):533-48. DOI: 10.1080/09553000802195331

[4] Słonina D, Biesaga B, Janecka A, Kabat D, Bukowska-Strakova K, Gasińska A. Low-dose hyper-radiosensitivity is not a common effect in normal asynchronous and G2-phase fibroblasts of cancer patients. International Journal of Radiation Oncology*Biology*Physics. 2014;88(2):369-76. DOI: 10.1016/j.ijrobp.2013.10.031

[5] Ghosh S, Kumar A, Chandna S. Connexin-43 downregulation in G2/M phase enriched tumour cells causes extensive low-dose hyper-radiosensitivity (HRS) associated with mitochondrial apoptotic events. Cancer Lett. 2015;363(1):46-59. DOI: 10.1016/j.canlet.2015.03.046

[6] Mathur A, Kumar A, Babu B, Chandna S. *In vitro* mesenchymal-epithelial transition in NIH3T3 fibroblasts results in onset of low-dose radiation hypersensitivity coupled with attenuated connexin-43 response. Biochim Biophys Acta Gen Subj. 2018;1862(3):414-26. DOI: 10.1016/j.bbagen.2017.11.013

[7] Pellegriti G, Frasca F, Regalbuto C, Squatrito S, Vigneri R. Worldwide increasing incidence of thyroid cancer: Update on epidemiology and risk factors. J Cancer Epidemiol. 2013;2013:965212. DOI: 10.1155/2013/965212

[8] Lim H, Devesa SS, Sosa JA, Check D, Kitahara CM. Trends in thyroid cancer incidence and mortality in the United States, 1974-2013. JAMA. 2017;317(13):1338-48. DOI: 10.1001/jama.2017.2719

[9] Mitchell AL, Gandhi A, Scott-Coombes D, Perros P. Management of thyroid cancer: United Kingdom National Multidisciplinary Guidelines. J Laryngol Otol. 2016;130(S2):S150-60. DOI: 10.1017/S0022215116000578

[10] Choi WJ, Kim J. Dietary factors and the risk of thyroid cancer: A review. Clin Nutr Res. 2014;3(2):75. DOI: 10.7762/cnr.2014.3.2.75

[11] Fagin JA. Genetics of papillary thyroid cancer initiation: Implications for therapy. Trans Am Clin Climatol Assoc. 2005;116:259-69; discussion 269-271. PMID: 16555619
[12] Furukawa K, Preston D, Funamoto S, Yonehara S, Ito M, Tokuoka S, et al. Long-term trend of thyroid cancer risk among Japanese atomic-bomb survivors: 60 years after exposure. Int J Cancer. 2013;132(5):1222-6. DOI: 10.1002/ijc.27749
[13] Naing S, Collins BJ, Schneider AB. Clinical behavior of radiation-induced thyroid cancer: Factors related to recurrence. Thyroid. 2009;19(5):479-85. DOI: 10.1089/thy.2008.0343
[14] Okegawa T, Pong RC, Li Y, Hsieh JT. The role of cell adhesion molecule in cancer progression and its application in cancer therapy. Acta Biochim Pol. 2004;51(2):445-57. PMID: 15218541
[15] Yang D, Louden C, Reinhold DS, Kohler SK, Maher VM, McCormick JJ. Malignant transformation of human fibroblast cell strain MSU-1.1 by (+-)-7 beta,8 alpha-dihydroxy-9 alpha,10 alpha-epoxy-7,8,9,10-tetrahydrobenzo [a]pyrene. Proc Natl Acad Sci U S A. 1992;89(6):2237-41. DOI: 10.1073/pnas.89.6.2237
[16] Du F, Zhao X, Fan D. Tumorigenicity Assay in Nude Mice. BIO-PROTOCOL [Internet]. 2017 [cited 2023 Mar 25];7(13). Available from: https://bio-protocol.org/e2364. DOI: 10.21769/BioProtoc.2364
[17] Ghosh S, Kumar A, Tripathi RP, Chandna S. Connexin-43 regulates p38-mediated cell migration and invasion induced selectively in tumour cells by low doses of γ-radiation in an ERK-1/2-independent manner. Carcinogenesis. 2014;35(2):383-95. DOI: 10.1093/carcin/bgt303
[18] Kumarswamy R, Seth RK, Dwarakanath BS, Chandna S. Mitochondrial regulation of insect cell apoptosis: Evidence for permeability transition pore-independent cytochrome-c release in the Lepidopteran Sf9 cells. Int J Biochem Cell Biol. 2009;41(6):1430-40. DOI: 10.1016/j.biocel.2008.12.009
[19] Howe B, Umrigar A, Tsien F. Chromosome preparation from cultured cells. J Vis Exp. 2014;(83):e50203. DOI: 10.3791/50203
[20] Joiner MC, Johns H. Renal damage in the mouse: The response to very small doses per fraction. Radiation Research. 1988;114(2):385. PMID: 3375433
[21] Musil LS, Goodenough DA. Biochemical analysis of connexin43 intracellular transport, phosphorylation, and assembly into gap junctional plaques. The Journal of Cell Biology. 1991;115(5):1357-74. DOI: 10.1083/jcb.115.5.1357
[22] Moh MC, Shen S. The roles of cell adhesion molecules in tumor suppression and cell migration: A new paradox. Cell Adh Migr. 2009;3(4):334-6. DOI: 10.4161/cam.3.4.9246
[23] Högnäs G, Hämälistö S, Rilla K, Laine JO, Vilkki V, Murumägi A, et al. Aneuploidy facilitates oncogenic transformation via specific genetic alterations, including Twist2 upregulation. Carcinogenesis. 2013;34(9):2000-9. DOI: 10.1093/carcin/bgt171
[24] Potapova TA, Zhu J, Li R. Aneuploidy and chromosomal instability: A vicious cycle driving cellular evolution and cancer genome chaos. Cancer Metastasis Rev. 2013;32(3–4):377-89. DOI: 10.1007/s10555-013-9436-6
[25] To-Ho KW, Cheung HW, Ling MT, Wong YC, Wang X. MAD2DeltaC induces aneuploidy and promotes anchorage-independent growth in human prostate epithelial cells. Oncogene. 2008;27(3):347-57. DOI: 10.1038/sj.onc.1210633
[26] Golubkov VS, Chekanov AV, Savinov AY, Rozanov DV, Golubkova NV, Strongin AY. Membrane type-1 matrix metalloproteinase confers aneuploidy and tumorigenicity on mammary epithelial cells. Cancer Res. 2006;66(21):10460-5. DOI: 10.1158/0008-5472.CAN-06-2997
[27] Morita T, Watanabe Y, Takeda K, Okumura K. Effects of pH in the *in vitro* chromosomal aberration test. Mutat Res. 1989;225(1–2):55-60. DOI: 10.1016/0165-7992(89)90033-x
[28] Adams T, Anwar R, Mfarej M, Rundatz T, Coyle M, McLaughlin J. Nutritional stress of cultured vero cells causes altered growth and morphology as seen in neoplastic transformation. AJUR [Internet]. 2015 Mar 27 [cited 2022 Aug 18];12(3). Available from: http://www.ajuronline.org/uploads/Volume%2012/Issue_3/AJURVol12Issue3May2015_pp_63_75.pdf
[29] Wünsch S, Gekle M, Kersting U, Schuricht B, Oberleithner H. Phenotypically and karyotypically distinct Madin-Darby canine kidney cell clones respond differently to alkaline stress. J Cell Physiol. 1995;164(1):164-71. DOI: 10.1002/jcp.1041640121
[30] Schneider DF, Chen H. New developments in the diagnosis and treatment of thyroid cancer: New Developments in Thyroid Cancer. CA A Cancer Journal for Clinicians. 2013;63(6):373-94. DOI: 10.3322/caac.21195
[31] Yu HM, Lee JM, Park KS, Park TS, Jin HY. Papillary thyroid carcinoma: Four cases required caution during long-term follow-up. Endocrinol Metab. 2013;28(4):335. DOI: 10.3803/EnM.2013.28.4.335
[32] Baum B, Georgiou M. Dynamics of adherens junctions in epithelial establishment, maintenance, and remodeling. J Cell Biol. 2011;192(6):907-17. DOI: 10.1083/jcb.201009141
[33] Ayollo DV, Zhitnyak IY, Vasiliev JM, Gloushankova NA. Rearrangements of the actin cytoskeleton and E-cadherin–based adherens junctions caused by neoplasic transformation change cell–cell interactions. Hartl D, editor. PLoS ONE. 2009;4(11):e8027. DOI: 10.1371/journal.pone.0008027
[34] Naus CC, Laird DW. Implications and challenges of connexin connections to cancer. Nat Rev Cancer. 2010;10(6):435-41. DOI: 10.1038/nrc2841

[35] Haerinck J, Berx G. Partial EMT takes the lead in cancer metastasis. Developmental Cell. 2021;56(23):3174-6. DOI: 10.1016/j.devcel.2021.11.012
[36] Liao C, Wang Q, An J, Long Q, Wang H, Xiang M, et al. Partial EMT in squamous cell carcinoma: A snapshot. Int J Biol Sci. 2021;17(12):3036-47. DOI: 10.7150/ijbs.61566
[37] Lambin P, Fertil B, Malaise EP, Joiner MC. Multiphasic survival curves for cells of human tumor cell lines: Induced repair or hypersensitive subpopulation? Radiat Res. 1994;138(1 Suppl):S32-36. PMID 8146321
[38] Lambin P, Marples B, Fertil B, Malaise EP, Joiner MC. Hypersensitivity of a human tumour cell line to very low radiation doses. International Journal of Radiation Biology. 1993;63(5):639-50. DOI: 10.1080/09553009314450831
[39] Iglesias ML, Schmidt A, Ghuzlan AA, Lacroix L, Vathaire F de, Chevillard S, et al. Radiation exposure and thyroid cancer: A review. Arch Endocrinol Metab. 2017;61(2):180-7. DOI: 10.1590/2359-3997000000257